# Diagnostic and Prognostic Potential of Multiparametric Renal MRI in kidney transplant patients

Rebeca Echeverria-Chasco [1,2], Paloma L. Martin-Moreno [2,3], Veronica Aramendia-Vidaurreta[1,2], Leyre Garcia-Ruiz[1,2], José María Mora-Gutiérrez [2,3], Marta Vidorreta [4], Arantxa Villanueva [2,5,6], David Cano[1,2], Gorka Bastarrika [1,2], Nuria Garcia-Fernandez [2,3,7], Maria A. Fernández-Seara [1,2]

[1.] Department of Radiology, Clínica Universidad de Navarra, Pamplona, Spain.
[2.] IdiSNA, Instituto de Investigación Sanitaria de Navarra.
[3.] Department of Nephrology, Clínica Universidad de Navarra, Pamplona, Spain.
[4.] Siemens Healthcare, Madrid, Spain
[5.] Electrical Electronics and Communications Engineering Department
[6.] Smart Cities Institute, Public University of Navarre, Pamplona, Spain
[7.] Red de Investigación Renal (REDINREN) and RICORS2040

## Supplementary Material

**SECTION 1: MRI Protocol**

- Arterial spin labeling:

Tissue blood flow was measured using a Pseudo-Continuous Arterial Spin Labeling (PCASL) sequence with a spin-echo echo planar imaging (SE- EPI) readout, following published consensus recommendations (1).

The PCASL labeling plane was placed around 8 cm above the center of the kidney, perpendicular to the aorta. The labeling was implemented with a train of short Hann-shaped radiofrequency pulses each lasting 500 μs, with 1 ms intervals and a flip-angle of 24.6º, resulting in a B1 average of 1.6 μT. The total labeling duration was 1.6 s. PCASL was unbalanced with a labeling average gradient (Gave) strength of 0.5 mT/m and a 6:1 slice-selective to average gradient ratio. Presaturation pulses selective to the imaging slices were applied at the beginning of the PCASL sequence to saturate the in-plane signal.

Background suppression (BS) pulses were employed to suppress the background tissue signal for a range of T1s between 1000–2500 ms. BS was implemented using a selective inversion Frequency Offset Corrected Inversion (FOCI) pulse prior to labeling, followed by two nonselective FOCI pulses after the labeling. The postlabeling delay (PLD) was 1.2 s. An M0 image (without presaturation, BS, or ASL labeling pulses) was acquired at the beginning of the ASL sequence, followed by 25 pairs of control-label images. The readout parameters were slice thickness = 5 mm (gap = 2.5 mm), acquisition matrix = 96 x 96, field of view (FOV) = 288 x 288 mm2, repetition time (TR) = 5000 ms, echo time (TE) = 23 ms, GRAPPA factor 2, 6/8 partial Fourier, bandwidth (BW) = 1890 Hz/pixel, and phase oversampling = 25%. Fat-suppression pulses were employed before the excitation pulses for each slice.

- Intravoxel incoherent motion

Intravoxel Incoherent Motion (IVIM) was acquired with a single-shot EPI readout following renal diffusion consensus guidelines (2). To separate the contribution of flow from pure diffusion, 13 b-values ranging from 0 to 800 s/mm2 were used: 0, 5, 10, 20, 30, 50, 70, 100, 200, 300, 400, 500, and 800 s/mm2. Eight low b-values were included to better characterize the fast signal decay. Monopolar gradients were applied in three orthogonal directions (three repetitions each) and acquisitions were subsequently averaged to minimize the effects of diffusion anisotropy. The readout parameters were slice thickness = 5 (gap = 2.5) mm, acquisition matrix = 128 x 128, FOV = 288 x 288 mm2, TR/TE = 5000/84 ms, GRAPPA factor = 2, BW = 1890 Hz/pixel, and phase oversampling = 25%. Fat-suppression (SPAIR) pulses were employed.

- T1 mapping

To measure the longitudinal relaxation time of kidney tissue, an inversion recovery sequence with an SE-EPI readout was employed, following published consensus recommendations (3). Fourteen inversion times (200, 300, 400, 500, 600, 700, 800, 900, 1000, 1200, 1400, 1600, 1800, and 2000 ms) were used with a TR = 5 s. The readout parameters matched those for the PCASL-SE-EPI sequence.

**SECTION 2: Regions of interest in renal cortical and medullary areas**

Supplementary Figure 1 shows representative segmentations of renal cortical (in red) and medullary (in blue) regions in one representative patient with inferior graft for the two MRI exams.

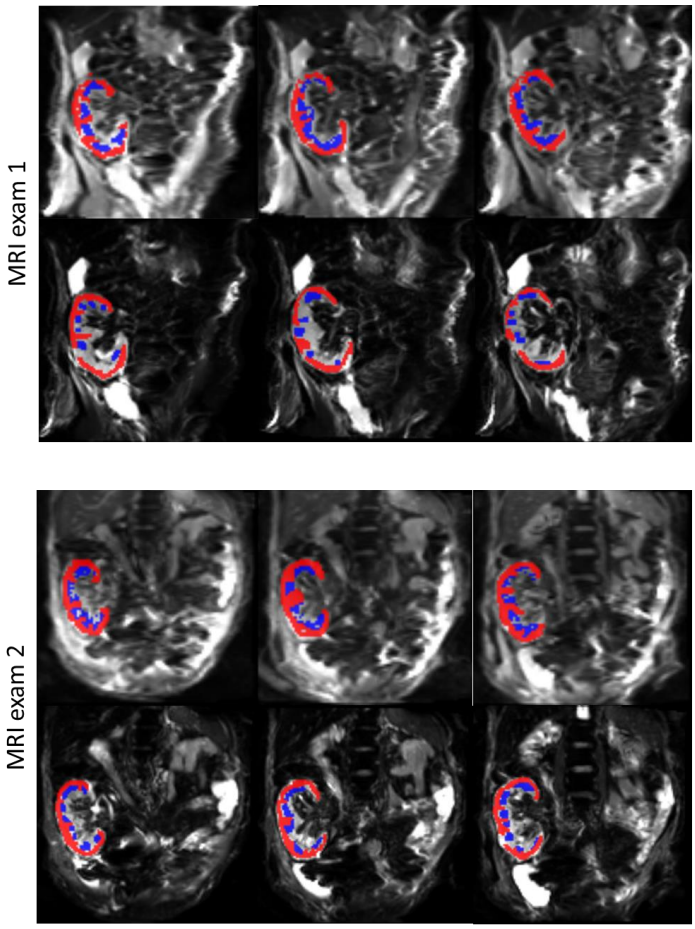


**Supplementary Figure 1:** Example of manually drawn regions of interest (ROIs) for cortex (in red) and medulla (in blue) in one representative patient with inferior graft function for the two MRI exams. Top row: ROIs drawn on the T1 maps have been overlaid on the M0 ASL image for the three slices. Bottom row: ROIs drawn on b=0 images have been overlaid on these images.

**SECTION 3: Variable Selection Process**

Methods:

A correlation analysis between MRI parameters (mean value of the two exams) was performed to detect highly correlated variables, excluding one of the parameters when correlations were stronger than 0.5. From the results of the correlation analysis, MRI parameters were selected to generate model 1. Then, a second model (model 2) was generated excluding variables D* and f due to poor reproducibility (within-subject coefficient of variation < 15%) according to the reproducibility results measured in previous work (4,5).

Results:

Supplementary Figure 2 shows the correlation matrix of MRI parameters, considering all patients, while Supplementary Figure 3 reports the value of Pearson's correlation coefficients and their associated p-values. Cortical ADC correlated strongly with coefficient D (r = 0.87) and with f (r = 0.74) and ΔADC correlated strongly with ΔD (r = 0.71), as expected. Considering these results, ADC and ΔADC were excluded from the multivariate regression models. Thus, model 1 included RBF, D, ΔD, D*, f, T1 and ΔT1. Subsequently, f and D* were excluded from model 2 due to poor reproducibility. Thus, model 2 included RBF, D, ΔD, T1 and ΔT1.

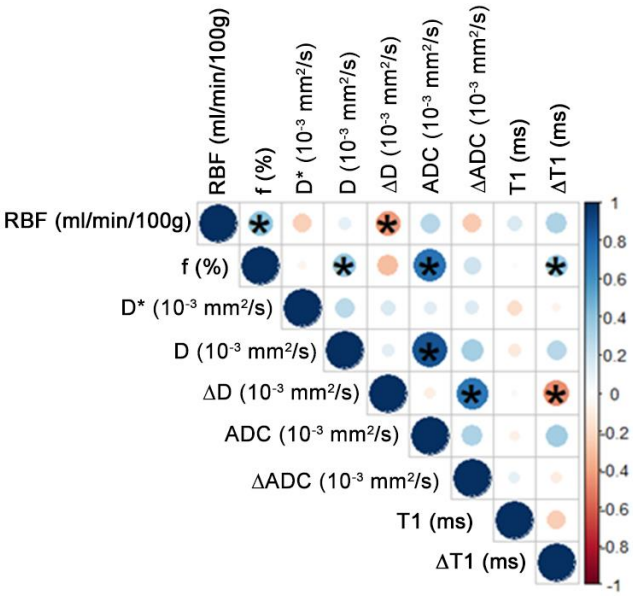


**Supplementary Figure 2**: Correlation matrix of MRI parameters (average value of exam 1 and 2). Positive correlations are displayed in blue while negative correlations are in red. Color intensity and circle size are proportional to correlation coefficients. Significant correlations are marked with '*'.

As shown in Supplementary Figure 3, the correlation between ASL derived RBF and diffusion derived f parameters was significant with r = 0.40 and p = 0.0248. Both parameters although evaluated with different imaging techniques contribute information related to tissue perfusion. However, ASL offers a quantitative measurement of renal blood flow while f is associated with the fast molecular movement caused by incoherent flow in the microvasculature or renal tubules.

| R | RBF (ml/min/100g) | f (%) | D* ($10^{-3}$ mm²/s) | D ($10^{-3}$ mm²/s) | ΔD ($10^{-3}$ mm²/s) | ADC ($10^{-3}$ mm²/s) | ΔADC ($10^{-3}$ mm²/s) | T1 (ms) | ΔT1 (ms) |
|---|---|---|---|---|---|---|---|---|---|
| RBF (ml/min/100g) | | 0.40 | -0.23 | 0.11 | -0.43 | 0.27 | -0.25 | 0.16 | 0.30 |
| f (%) | | | -0.06 | 0.37 | -0.31 | 0.74 | 0.21 | 0.02 | 0.36 |
| D* ($10^{-3}$ mm²/s) | | | | 0.26 | 0.15 | 0.12 | 0.14 | -0.17 | -0.06 |
| D ($10^{-3}$ mm²/s) | | | | | 0.12 | 0.87 | 0.33 | -0.11 | 0.28 |
| ΔD ($10^{-3}$ mm²/s) | | | | | | -0.09 | 0.71 | 0.03 | -0.47 |
| ADC ($10^{-3}$ mm²/s) | | | | | | | 0.30 | -0.07 | 0.35 |
| ΔADC ($10^{-3}$ mm²/s) | | | | | | | | 0.10 | -0.10 |
| T1 (ms) | | | | | | | | | -0.25 |
| ΔT1 (ms) | | | | | | | | | |

| p | RBF (ml/min/100g) | f (%) | D* ($10^{-3}$ mm²/s) | D ($10^{-3}$ mm²/s) | ΔD ($10^{-3}$ mm²/s) | ADC ($10^{-3}$ mm²/s) | ΔADC ($10^{-3}$ mm²/s) | T1 (ms) | ΔT1 (ms) |
|---|---|---|---|---|---|---|---|---|---|
| RBF (ml/min/100g) | | 0.0248 | 0.2006 | 0.5655 | 0.0138 | 0.1333 | 0.1615 | 0.3891 | 0.0933 |
| f (%) | | | 0.7512 | 0.0369 | 0.0846 | 0.0000 | 0.2516 | 0.9009 | 0.0459 |
| D* ($10^{-3}$ mm²/s) | | | | 0.1479 | 0.3971 | 0.5058 | 0.4326 | 0.3519 | 0.7419 |
| D ($10^{-3}$ mm²/s) | | | | | 0.5202 | 0.0000 | 0.0629 | 0.5397 | 0.1219 |
| ΔD ($10^{-3}$ mm²/s) | | | | | | 0.6298 | 0.0000 | 0.8638 | 0.0067 |
| ADC ($10^{-3}$ mm²/s) | | | | | | | 0.0901 | 0.6922 | 0.0517 |
| ΔADC ($10^{-3}$ mm²/s) | | | | | | | | 0.5754 | 0.6023 |
| T1 (ms) | | | | | | | | | 0.1755 |
| ΔT1 (ms) | | | | | | | | | |

**Supplementary Figure 3**: Matrix with Pearson's correlations (top) and associated p-values (bottom) obtained from all MRI quantitative parameters measured in the cortex. Significant correlations are highlighted in green.

**SECTION 4: Delayed Graft Function**

We evaluated whether belonging to the "delayed graft function" group is related to belonging to the "inferior graft function" group or not, with Fisher's Exact Test for Count Data:

**a) Delayed Graft Function, criterion 1**

| | IGF | SGF | N |
|---|---|---|---|
| **DGF** | **3** | **1** | 4 |
| **EGF** | **7** | **21** | 28 |
| | 10 | 22 | 32 |

p-value = 0.07925

**b) Delayed Graft Function, criterion 2**

| | IGF | SGF | N |
|---|---|---|---|
| **DGF** | **5** | **5** | 10 |
| **EGF** | **5** | **17** | 22 |
| | 10 | 22 | 32 |

p-value = 0.2168

**SECTION 5:**

Supplementary Table 1: Demographic and Biopsy Data

| | | | | | | Donor biopsy | | | | | Biopsy first week post-transplant | | | | |
|---|---|---|---|---|---|---|---|---|---|---|---|---|---|---|---|
| ID | Age (years) | Sex (M/F) | Donor Age (years) | Donor Sex (M/F) | Donor Type (A/BD) | Glomerular Sclerosis % | Tubular atrophy % | Interstitial fibrosisl % | Arteriolar Hyalinosis | Inflammatory infiltrates | Glomerular Sclerosis % | Tubular atrophy % | Interstitial fibrosisl % | Arteriolar Hyalinosis | Inflammatory infiltrates |
| 1 | 47 | M | 43 | M | BD | | | | | | | | | | |
| 2 | 58 | F | 40 | M | BD | 0 | 0 | <10 | 0 | | | | | | |
| 3 | 77 | M | 64 | F | BD | 0 | 0 | <10 | 0 | | | | | | |
| 4 | 61 | M | 69 | M | BD | 12 | 30 | 30 | 0 | | 14 | 20 | 20 | 0 | Dense, polymorphonuclear |
| 5 | 56 | M | 64 | M | BD | 10 | 0 | 0 | 0 | | | | | | |
| 6 | 28 | F | 59 | F | CD | | | | | | | | | | |
| 7 | 40 | F | 25 | F | BD | | | | | | | | | | |
| 8 | 41 | M | 53 | M | BD | | | | | | | | | | |
| 9 | 71 | M | 45 | M | BD | 0 | 0 | 10 | 0 | | | | | | |
| 10 | 38 | M | 52 | F | BD | | | | | | | | | | |
| 11 | 49 | F | 49 | M | CD | 0 | 0 | 0 | <10 | | | | | | |
| 12 | 66 | F | 71 | F | BD | 4 | 0 | 0 | 0 | | | | | | |
| 13 | 62 | M | 57 | M | CD | 8 | 0 | 0 | 0 | | 0 | 0 | 0 | 0 | <25% with lymphocytes and histiocytes |
| 14 | 66 | M | 45 | F | CD | 0 | 0 | 0 | 0 | | | | | | |
| 15 | 58 | M | 54 | F | BD | | | | | | | | | | |
| 16 | 54 | M | 47 | M | CD | | | | | | | | | | |
| 17 | 73 | M | 68 | M | BD | 7 | 0 | 0 | 0 | | | | | | |
| 18 | 67 | F | 71 | F | CD | 0 | <10 | <10 | 0 | | | | | | |
| 19 | 31 | F | 51 | M | BD | | | | | | | | | | |
| 20 | 51 | M | 51 | M | BD | 0 | <10 | 0 | 0 | | | | | | |
| 21 | 29 | F | 47 | F | CD | | | | | | | | | | |
| 22 | 45 | M | 47 | F | CD | | | | | | | | | | |
| 23 | 64 | M | 50 | F | CD | | | | | | | | | | |
| 24 | 51 | F | 66 | M | BD | 12 | 0 | 0 | 0 | | | | | | |
| 25 | 51 | M | 61 | F | CD | | | | | | | | | | |
| 26 | 26 | M | 59 | F | BD | | | | | | | | | | |
| 27 | 67 | F | 34 | M | CD | | | | | | | | | | |
| 28 | 45 | M | 34 | M | CD | | | | | | 5 | 10 | 10 | 0 | 10% lymphocytes |
| 29 | 78 | M | 78 | M | CD | 9 | 0 | 0 | 0 | | | | | | |
| 30 | 78 | F | 78 | M | CD | | | | | | | | | | |
| 31 | 50 | F | 41 | M | BD | | | | | | | | | | |
| 32 | 33 | M | 48 | F | BD | 2 | 0 | 0 | 0 | | | | | | |
| Mean | 53.47 | F, n = 12 | 53.78 | F, n = 18 | CD, n = 14 | | | | | | | | | | |
| SD | 14.95 | M, n= 20 | 12.67 | M, n = 14 | BD, n = 18 | | | | | | | | | | |

M: Male, F: Female, CD: Circulatory Death, BD: Brain Death

**REFERENCES**


[1] Nery F, Buchanan CE, Harteveld AA, et al. Consensus-based technical recommendations for clinical translation of renal ASL MRI. Magn Reson Mater Physics, Biol Med. 2020;33(1):141-161

[2] Ljimani A, Caroli A, Laustsen C, et al. Consensus-based technical recommendations for clinical translation of renal diffusion-weighted MRI. Magn Reson Mater Physics, Biol Med. 2020;33(1):177-195.

[3] Dekkers IA, de Boer A, Sharma K, et al. Consensus-based technical recommendations for clinical translation of renal T1 and T2 mapping MRI. Magn Reson Mater Physics, Biol Med. 2020;33(1):163-176.

[4] Echeverria-Chasco R, Martin-Moreno PL, Garcia-Fernandez N, Vidorreta M, Aramendia-Vidaurreta V, Cano D, et al. Multiparametric renal magnetic resonance imaging: A reproducibility study in renal allografts with stable function. NMR Biomed 2023;36:e4832. https://doi.org/10.1002/nbm.4832.

[5] Bane O, Hectors S, Gordic S, Kennedy P, Wagner M, Weiss A, et al. Multiparametric magnetic resonance imaging shows promising results to assess renal transplant dysfunction with fibrosis. Physiol Behav 2020;97:414–20. https://doi.org/10.1016/j.kint.2019.09.030.Multiparametric.